

# The CMS High Granularity Calorimeter Scintillator/SiPM Tileboards

**Mathias Reinecke** *on behalf of the CMS collaboration*

Deutsches Elektronen-Synchrotron DESY, 22607 Hamburg, Germany

Email: mathias.reinecke@desy.de

**Abstract.** The new CMS High Granularity Calorimeter (HGCAL), being built for HL-LHC, will have unprecedented transverse and longitudinal readout and trigger segmentation. In regions of low radiation, HGCAL will be equipped with small plastic scintillator tiles as active material coupled to on-tile silicon photomultipliers. With respect to earlier developments targeted at a future e+e- collider, additional challenges in terms of radiation hardness, data rates and mechanical integration including cooling need to be addressed. We will present the evolving design, results on the performance of irradiated SiPMs, the optimisation of scintillator tiles, the status of active element prototypes with integrated electronics, and the preparations for automated production.

## 1. Operational Environment of the Scintillator Tileboards

For the high-luminosity phase of the LHC (HL-LHC) at CERN the calorimeter of the CMS detector will be upgraded. As part of the upgrade two new endcaps will be installed, containing a novel calorimeter with unprecedented transverse and longitudinal granularity [1]. Each of the new high-granularity calorimeter (HGCAL) endcaps (Fig. 1) contains 26 layers ( $2 \times 13$ , double sided) of electromagnetic (CE-E) and 21 layers of hadronic calorimeter (CE-H). In the front and inner region, the detector layers are realized by hexagonal-shaped silicon modules with in total 6 million detector channels in about  $620\text{m}^2$  of silicon. In the back region two technologies are combined with hexagonal silicon modules at the inner part and trapezoidal-shaped scintillator modules in the outer part. The scintillator detector modules are based on individually wrapped plastic scintillator tiles and silicon photomultipliers (SiPMs) with in total 240,000 detector channels and a scintillator area of about  $400\text{m}^2$ . Detailed information on the HGCAL project is shown in [2, 3], this contribution focuses on the development of the scintillator detector modules.

For the development of the scintillator modules and the corresponding electronics, the operating conditions within the CMS endcaps have to be considered. When an integrated luminosity of  $3000\text{fb}^{-1}$  is reached at CMS, the scintillator modules especially at the inner radii will have been exposed to neutron fluences of up to  $5 \times 10^{13}\text{neq/cm}^2$  and a total ionizing dose of 200krad. The boundary between silicon and scintillator detector (cf. Fig. 1) is defined by the irradiation levels and where they allow the operation of SiPMs. To compensate irradiation effects, the detector modules in the endcaps will be operated at  $-30^\circ\text{C}$ . The magnetic field can reach 3.8T in the endcaps, prohibiting the use of magnetic materials and magnetic-sensitive components.

In the proposed detector concept for the CMS endcaps 36 tileboards are placed next to each other, following the circular structure of the endcaps around the beampipe. In radial direction perpendicular to



the beampipe, up to 5 tileboards are placed next to each other, forming a basic  $10^\circ$  detector unit. Scintillator and silicon detector modules are assembled into common cassettes, each cassette covering  $60^\circ$  (Fig. 2). Six cassettes close the ring around the beampipe in the layers.

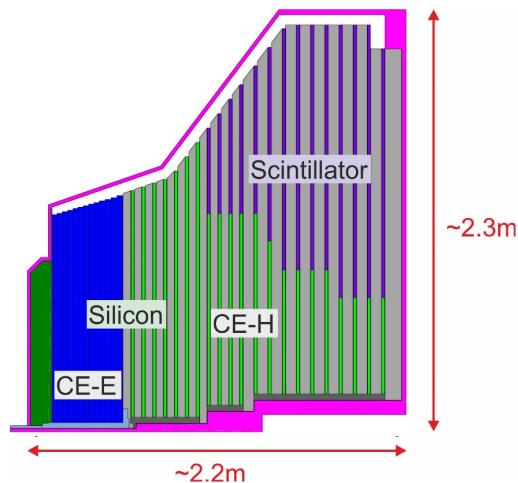


**Figure 1.** Cross-sectional view to an endcap of the proposed new CMS high-granularity calorimeter (HGCal).

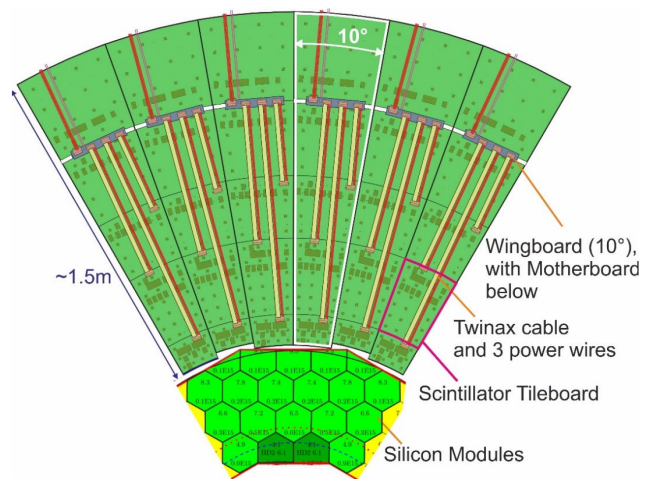


**Figure 2.** Top view to a mixed  $60^\circ$  cassette of a detector layer, including scintillator tileboards (top) and silicon modules (bottom).

In the detector cassettes the tileboards are mounted onto a 6mm-thick copper heatsink that defines the operating temperature of  $-30^\circ\text{C}$ . For the tileboard components on the heatsink side, corresponding cavities are machined into the heatsink. Within a basic  $10^\circ$  detector element, all signals to and from the tileboards as well as the power are exclusively provided through a single connector. Twin-axial cables for the fast differential signals and individual wires for the supply voltages connect the tileboards to the wingboards and motherboards that interface to the off-detector power supplies and data acquisition.

## 2. Scintillator Tileboards and their Large-Scale Production

### 2.1. Scintillator Tileboards

In the scintillator detector 8 major geometries of tileboards cover all positions in the  $10^\circ$  detector units (cf. Fig. 2) and the different layers. The tileboard sizes range from about  $21 \times 15 \text{cm}^2$  to  $45 \times 42 \text{cm}^2$ , the tileboard PCBs have 8 layers for power and signal routing and a total thickness of about 1.2mm. A typical tileboard as shown in Fig. 3 has 64 detector channels, the number of channels varies from 48 to 96 for the different board sizes. Main component for the read out of the SiPMs is the analogue / digital ASIC HGCROC for up to 72 detector channels [4]. In order to limit the supply currents to the tileboards, two step-down DC-DC converters bPOL12 [5] form the power input to the tileboards with 10V input voltage and the output voltages of 1.5V and 3.3V. All noise sensitive supply voltages for the HGCROC and the SiPMs are generated from linear regulators. The SiPM bias voltage is provided by the new ASIC development ALDOv2 [6]. All slow control tasks as the configuration of the HGCROCs, the monitoring of supply voltages, temperatures and SiPM bias voltages are performed by a GBT\_SCA [7] on the tileboards.

The tileboard side opposite to the components contains except for the connector to the DAQ and five mounting bolts the individually wrapped scintillating tiles (cf. Fig. 3) only. The tiles have a centred, spherical cavity for the SiPMs. For each channel, an ultraviolet LED is placed next to the SiPMs as part of the calibration- and gain-monitoring system. During a calibration sequence, the LEDs send in parallel to all channels of a tileboard an optical pulse of typically 6ns width into the scintillating tiles. The LED system is triggered by the HGCROC, ensuring the synchronous generation of the optical pulses to the

HGCROC data taking clock. The amplitude of the LEDs can be adjusted by a single, external DC voltage from the motherboard.

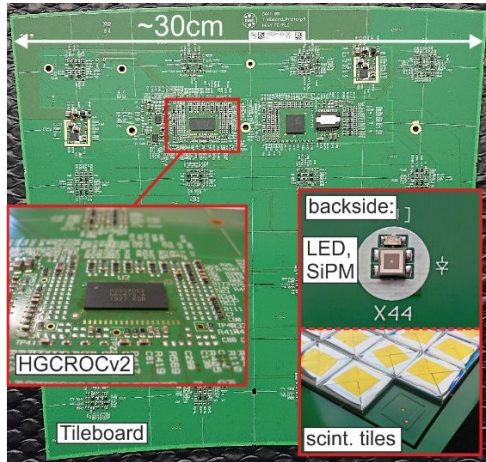


**Figure 3.** Scintillator tileboard with main components on top and SiPMs, LEDs and scintillating tiles on back side.

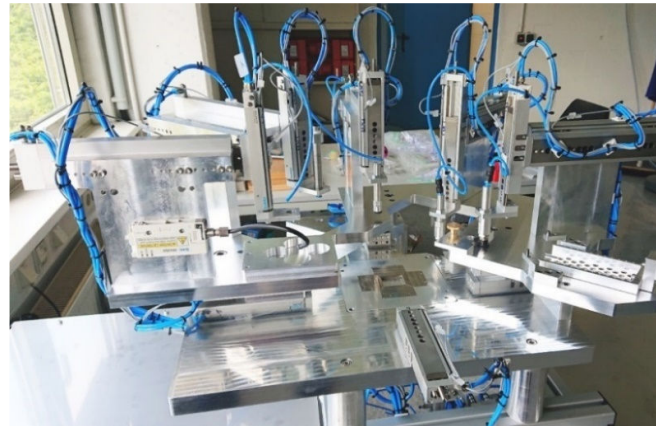


**Figure 4.** Wrapping station with air-pressure induced, translationally moving wrapping elements.

## 2.2. Large Scale Production of Scintillator Tiles and Tile Assembly

For the 240,000 detector channels on almost 3800 tileboards in the scintillator detector, efficient and reliable production and assembly procedures are required. While for the assembly of the surface-mount components standard techniques can be applied, new procedures have been developed for the individual wrapping of the scintillator tiles into reflector foil and the mounting of the wrapped tiles to the tileboards.

For the tile wrapping, a dedicated wrapping station has been developed (Fig. 4). The center part of the wrapping station can be replaced to be operational for the trapezoidal shaped, 3mm thick tiles in 21 different sizes, ranging from  $23 \times 23 \text{mm}^2$  to  $55 \times 55 \text{mm}^2$ . For a better position reproducibility, only translational movements of the wrapping elements have been implemented, initiated by air-pressure and the control of the respective valves by a programmable unit. With the wrapping station a throughput of three to four tiles per minute can be achieved.

After wrapping, the tiles are glued to the tileboards by a standard pick-and-place (P&P) station (Yamaha I-Pulse). In a first step with a special dispenser head mounted to the P&P station the glue is applied to all tile positions on the tileboards. In a second step, all tiles are mounted to the tileboards followed by a 24h glue-curing phase at room temperature. With the P&P station, 20 tileboards can be assembled per day.

## 3. Results from Testbench and Test-Beam Campaigns

The first tileboard prototypes have been tested extensively in the lab and in test-beam campaigns at the 3GeV electron test-beam facility at DESY and the 120GeV proton test-beam facility at Fermilab.

### 3.1. Results from Testbench

For the noise measurement a tileboard with different types of SiPMs assembled to the board was used. The achieved noise as shown in Fig. 5 for all channels depends as expected on the HGCROC gain and the capacitance (area) of the SiPM connected to the respective channel. Channels without assembled SiPMs show the lowest noise. For the aimed, final type of SiPMs (cf. IV and III in Fig. 5) the noise is below two 10-bit ADC counts for high gain settings and below 1.2 ADC counts for low gains that are used in normal operation for physics data taking. The measured noise on the tileboards corresponds to the results achieved on the dedicated test-modules for HGCROC characterizations.

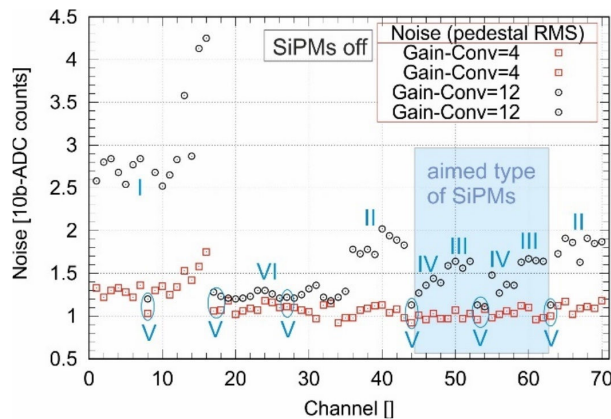


**Figure 5.** Noise on a tileboard for high and low gain setting of the HGCROC (Gain-Conv). The noise in a channel also depends on the area of the connected SiPM (I, II, III, IV). Channels without assembled SiPMs (V, VI) have lowest noise.

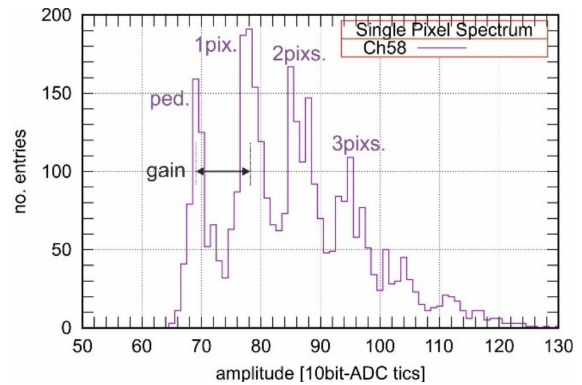


**Figure 6.** Typical Single Pixel Spectrum (SPS) obtained on a tileboard with the integrated LED system at 4V overvoltage of the SiPMs.

The noise has to be considered with respect to the smallest signals that have to be detected in the scintillator detector: The single-pixel spectra (SPS) of the SiPMs as shown in Fig. 6. For SPS measurements the integrated LED system of the tileboards is used. At low light intensities in the tiles, no or very few pixels of the SiPMs are excited. In the resulting SPS the distances of the individual peaks are a measure of the overall channel gain, including the gains of the SiPMs and the HGCROCs. The SPS is measured for calibration and gain monitoring for each channel. By repetitive measurements at low rate as e.g. twice per day, drifts of temperature and bias voltage can be identified and be corrected for. With typical distances of the SPS peaks of 8-11 ADC counts at 4V SiPM overvoltage and a noise below 2 ADC counts at high gain (cf. Fig. 5), a good signal-to-noise ratio of at least 4 has been achieved.

### 3.2. Results from Test-beam Campaigns

With respect to the irradiation levels at CMS, the SiPMs in the most critical, inner areas of the endcaps are affected most. When the integrated luminosity finally reaches  $3000\text{fb}^{-1}$  at CMS, the SiPM's dark count rate (DCR) will have increased to a few GHz and leakage currents of up to 1mA are expected for the larger  $4\text{mm}^2$  SiPMs. The increased leakage currents lead to a self-heating of the devices and together with the irradiation damage to an increase of the SiPM breakdown voltages.

In dedicated tests at the 3GeV electron test-beam facility at DESY with irradiated SiPMs mounted onto a tileboard the influence of the irradiation is characterized. For these tests at room temperature, the SiPMs have been irradiated with a neutron fluence of  $2 \times 10^{12}\text{neq/cm}^2$ , equivalent to the maximum expected fluence of  $5 \times 10^{13}\text{neq/cm}^2$  at  $-30^\circ\text{C}$ . A first, preliminary result for minimum-ionizing particles (MIPs) is shown in Fig. 7. Although the final signal-to-noise (S/N) value for MIPs and irradiated SiPMs is still under analysis, the results already show that MIPs can be well resolved for worst-case irradiation conditions in the scintillator detector. To optimize the performance, important operating parameters as the environmental temperature and the SiPM overvoltage (Fig. 7: 2V overvoltage) are still under discussion.

For the detection of MIPs in the scintillator detector a minimum S/N of above 5 is aimed at the end of the experiment's lifetime and in all SiPM positions. The critical areas to reach this are the inner radii of the scintillator detector in the endcaps with the highest irradiation doses. Next to the described effects for the SiPMs, a reduced light yield is expected from the scintillator tiles from irradiation.

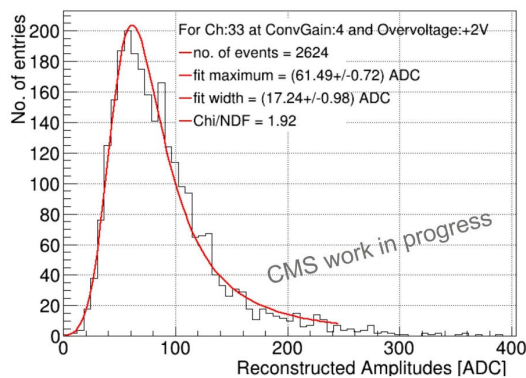


**Figure 7.** Minimum-Ionizing Particle (MIP) peak of an irradiated SiPM, obtained with a tileboard at the 3GeV electron test-beam facility at DESY.

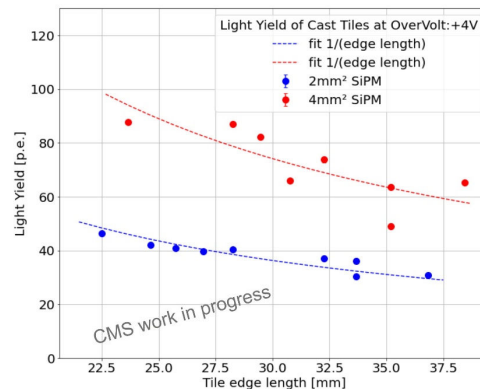


**Figure 8.** Light Yield for cast scintillator tiles of different sizes and 2mm<sup>2</sup> and 4mm<sup>2</sup> SiPMs.

To compensate for irradiation effects larger SiPMs with areas of 4mm<sup>2</sup> compared to 2mm<sup>2</sup> will be used in areas with high irradiation levels, resulting in a by two-times higher light yield as shown in Fig. 8. In addition, cast scintillators are used instead of moulded scintillators, which have a higher light yield by a factor of about 2 at the cost of a higher price. As a benefit, in the inner areas of the endcaps with the highest irradiation levels the smallest tiles are located which have a higher light yield (cf. Fig. 8). To optimize the detector's performance, studies on scintillator material, tile wrapping and SiPM parameters are still ongoing.

#### 4. Conclusion

For the high-luminosity phase of the LHC at CERN (HL-LHC) the CMS calorimeter endcaps will be replaced. In the outer region of the endcaps, a scintillator detector based on SiPMs and individually wrapped, plastic scintillator tiles will be implemented. A harsh radiation environment, a high magnetic field up to 3.8T and an operating temperature of -30° define strong requirements on the detector modules. The proposed scintillator detector concept has been verified in dedicated tests in the lab and in test-beam campaigns and is in the final optimization phase. For the production of the about 4000 modules with 240,000 channels, automated production techniques are in final preparation.

#### References

- [1] CMS collaboration 'The Phase-2 Upgrade of the CMS Endcap calorimeter', Technical Design Report, CERN-LHCC-2017-023, CMS-TDR-019, 2018
- [2] T. Quast 'Status and plans for the CMS High Granularity Calorimeter upgrade project', parallel talk, TIPP 2021 conference, 2021
- [3] M. Noy 'Electronics and Triggering Challenges for the CMS High-Granularity Calorimeter', parallel talk, TIPP 2021 conference, 2021
- [4] D. Thienpont 'HGCROC: the front-end readout ASIC for the CMS High Granularity Calorimeter', plenary talk, TIPP 2021 conference, 2021
- [5] F. Faccio 'The bPOL12V DCDC converter for HL-LHC trackers: towards production readiness', TWEPP conference 2019
- [6] Paolo Carniti et al. 'ALDOv2, a multi-purpose linear regulator for the CMS Barrel Timing Layer detector', ACES 2020 workshop, 2020
- [7] A. Caratelli et al. 'The GBT-SCA, a radiation tolerant ASIC for detector control and monitoring applications in HEP experiments', TWEPP conference 2015